

On the high resolution content of elemental maps

C J D Hetherington¹, C B Boothroyd², R E Dunin-Borkowski² and J L Hutchison¹

¹ Department of Materials, Parks Road, Oxford OX1 3PH

² Department of Materials Science and Metallurgy, Pembroke Street, Cambridge CB2 3QZ

ABSTRACT: Elemental maps formed from electron spectroscopic images can show detail that is apparently on the atomic scale. A number of techniques are proposed for investigating whether such contrast is truly “compositional” in nature. Initial results from a model tungsten sulphide sample are described.

1. INTRODUCTION

Two-dimensional elemental maps of materials can now be formed routinely from electron spectroscopic images acquired in an energy-filtering transmission electron microscope. Recently, several authors (e.g. Hashimoto et al., 1997; Freitag and Mader, 1999) demonstrated that elemental maps of crystalline samples can show lattice fringes. However, it is not readily appreciated that the contrast in such fringes may not always represent the true chemical distribution of the element of interest. Instead, it may result from elastic scattering in the sample following the inelastic scattering event. In this paper, we propose a series of experiments that can be used to distinguish between chemical and “elastic” lattice fringe contrast in an elemental map. (We note however that there is a continuous gradation from fine microstructure to lattice fringes; our discussion is applicable to any form of elemental map). We illustrate our approach through the examination of a sample of a tungsten sulphide, in which adjacent WS_2 {002} layers have a spacing of 0.618 nm and consist of double atomic layers of S sandwiched between single layers of W.

2. ENERGY SELECTED IMAGES AND ELEMENTAL MAPS

Figure 1 shows three energy-selected images of WS_2 lattice fringes, in which atomic resolution detail is present in the energy-loss images as well as in the zero-loss image. Similar images have been presented by Boothroyd (1998). Such contrast is dominated by elastic scattering in the sample (following the inelastic event). As the energy loss increases, so the degree of angular scattering in the sample (and therefore the effective beam convergence in the image) increases. Thus, at low energy loss the contrast may reverse with defocus, whereas at high energy loss there may be no contrast reversals and the image may be mostly incoherent. If a background subtracted elemental map is formed from images obtained at several energy losses close to that of a S L or a W O core shell edge, the contrast is ideally proportional to the local concentration of S or W projected in the beam direction. In practice, however, the contrast also depends on the cross-section for core-loss scattering, on absorption by other atoms and on elastic scattering in the sample.

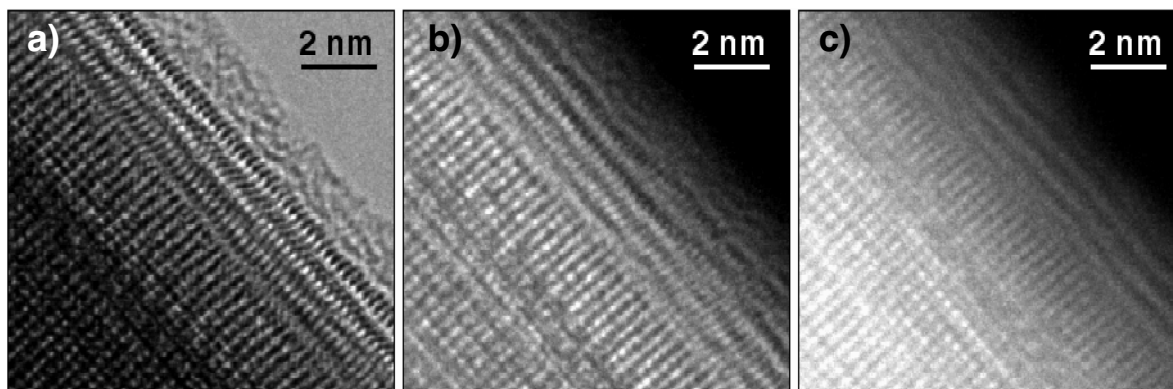


Figure 1. a) 0 eV, b) 30 eV and c) 90 eV loss lattice fringe images of WS_2 layers (top right) adjacent to a W oxide crystal (bottom left).

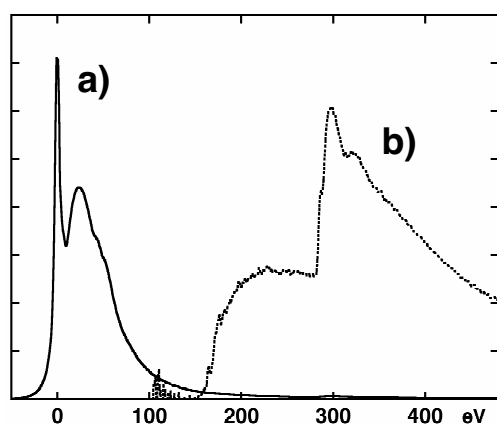
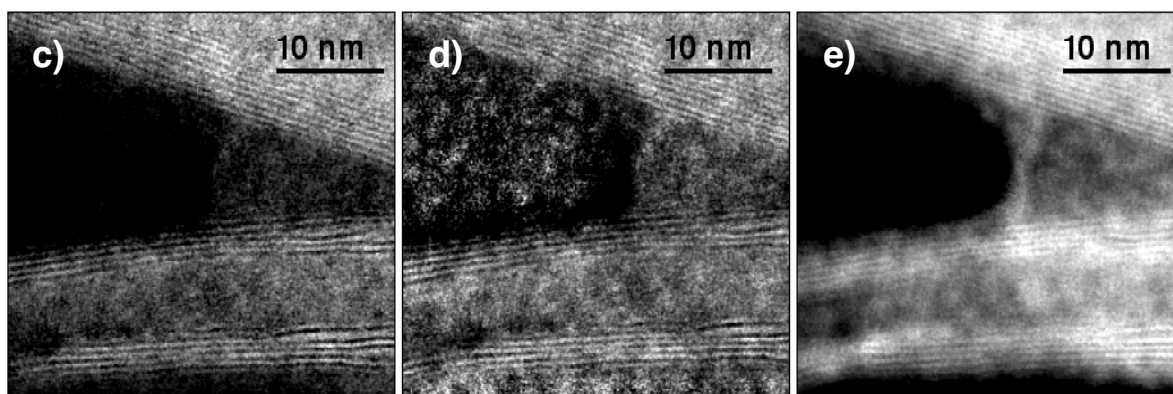


Figure 2. Energy loss spectra obtained from the edge of a WS_2 coated particle showing a) the W O_{23} edge at 36 eV and the W O_1 edge at 77 eV, and b) the S L_{23} edge at 165 eV after background subtraction from the spectrum shown in a; c) S elemental map obtained from WS_2 nanotube using the three window method; d) S elemental map divided by its background; e) Background used to generate c and d.



The spatial resolution of the chemical information in an energy loss image is determined by parameters such as the delocalisation of the inelastic scattering event. Equations given by Krivanek et al. (1995) predict delocalisations of 2.66 nm for the W O edge at 36 eV, 0.69 nm for the S L edge at 165 eV, 0.10 nm for the W M edge at 1809 eV and 0.08 nm for the S K edge at 2472 eV. The positions of some of these edges can be seen in the experimental energy loss spectra shown in Figs. 2a and 2b. If the delocalisation is larger than the lattice fringe spacing (0.618 nm in the present sample) then the elemental map should show no lattice fringes.

A three window background subtracted elemental map is obtained by subtracting a background from the core loss signal. This background is usually estimated using a power law model from two images acquired prior to the edge. If there is no chemical information associated with the edge then the map and the background are, to a good approximation, multiples of each other. Although the background signal may show lattice fringes that are related to a normal high resolution image of the structure, the same will be true of the signal from the energy loss of interest, and so a three window elemental map may show lattice

fringes even when there is no chemical signal. In contrast, a "ratio image" calculated by dividing the core loss signal by the background should show no lattice fringes. Figures 2c – 2e show such images obtained from a WS₂ nanotube close to the S L edge. As predicted, the elemental map shown in Fig. 2c shows lattice fringes. The ratio of the core loss edge divided by the background shown in Fig. 2d still contains lattice fringes, suggesting that true chemical information may be present. However, care is required because there are other reasons why lattice fringes may appear in an image such as that shown in Fig. 2d. For example, all of the different energy loss images must be perfectly aligned; a very slight misregistration of a fraction of a lattice fringe will be amplified by any extrapolation and subtraction process. Even if the alignment is perfect, a slight change in the sample drift rate can cause one image to be blurred more than the others and an error in the resulting map. Experimentally, the microscope accelerating voltage is usually changed between the different energy loss images in order to ensure that the sample remains in focus. However, this change in voltage can change the area illuminated on the specimen, altering the relative intensities of the three images. Finally, the background image estimated by extrapolation will be slightly different from the true background image as the increased angular scattering with energy loss will change the image detail slightly, particularly if the image is not perfectly in focus.

3. OMEGA-R IMAGES

A possible way to overcome the alignment problem is to collect omega-r images by placing a slit over the entrance of the imaging filter perpendicular to the dispersion direction, and then adjusting the quadrupole settings in spectrometer mode to spread the spectrum over the full width of the detector. This gives an image in which the x direction represents energy loss and the y direction distance on the specimen. Two examples are shown in Fig. 3. Unfortunately, the effects of chromatic aberration are now apparent and, although the objective focus can be adjusted to bring a particular edge into focus, contrast reversals are apparent at energy losses on either side of this edge. (This is of course the reason why the microscope accelerating voltage is changed when collecting energy loss images).

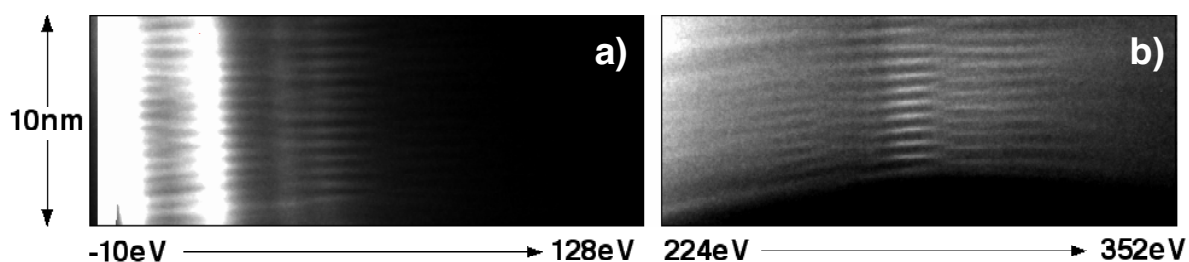


Figure 3. Omega-r maps across two WS₂-coated particles, for a dispersion of 0.3 eV/pixel. a) shows the zero loss, plasmon loss and the W O₂₃ and W O₁ edges, whereas b) was obtained around the C K edge. In addition to the contrast reversals, the fringes go out of focus away from the C edge.

4. LINESCANS

The only method that can be used to overcome the problems of alignment and chromatic aberration is to collect a linescan of energy loss spectra across the lattice fringes with the probe focused on the specimen. Chromatic aberration then simply blurs the width of the spectrum on the detector and all of the electrons come from the point on the specimen illuminated by the probe. In addition, it is possible to collect a high angle annular dark field (HAADF) linescan simultaneously, providing an unambiguous measurement of the position of the heavier W layers. Such linescans are shown in Fig. 4 alongside an

HAADF image of the area they were taken from. The specimen thickness increases from left to right in Fig. 4b, and it is just possible to make out about 6 lattice fringes in the HAADF trace between 2 and 5 nm. The disadvantages of such linescans include the build-up of C contamination and noise resulting from each probe position having a slightly different exposure time and/or dose of electrons, making the fringes difficult to distinguish.

Neither of the core loss/background traces shows convincing lattice fringes, given that the delocalisation is about the same as the lattice fringe separation (0.69 nm) for S L and is much bigger (2.66 nm) for W O. However, both traces, especially the W O trace, are noisy and indeed few lattice fringes were visible in any of the pre- or post-edge images, despite such fringes being clearly visible in the TEM (Fig. 2e) and in omega-r images (Fig. 3b).

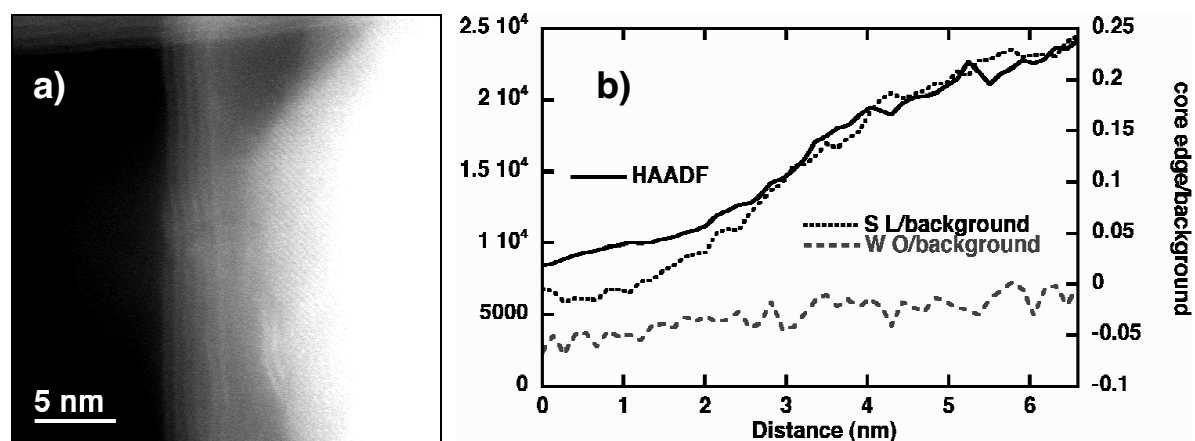


Figure 4. a) HAADF image of area linescans came from; b) HAADF linescan and corresponding plots of the (S L edge)/(S L background) and (W O edge)/(W O background) intensity.

5. CONCLUSIONS

The resolution limit of elemental maps obtained in TEM is for most purposes limited by alignment and drift. It is therefore difficult to produce an elemental map that contains lattice fringes and to expect them to contain compositional information on an atomic scale. In principle, it should be possible to use linescans of energy loss spectra to unambiguously record elemental maps without alignment problems. However, contamination, noise and the instrumental dead time associated with collecting spectra in series using a fine probe provide a new set of problems. WS₂ is worth further investigation as the delocalisation of the W M (1809 eV) and S K (2472 eV) edges is low enough for lattice fringes to be resolved, while lattice fringes should not be resolved (or only just resolved) for the W O and S L edges.

ACKNOWLEDGMENTS

We are grateful to Prof. R Tenne and Dr J Sloan for provision of the WS sample.

REFERENCES

- Boothroyd CB 1998, *J. Microsc.* **190**, 99
 Freitag B and Mader W 1999, *J. Microsc.* **194**, 42
 Hashimoto H, Luo ZP, Kawasaki M, Hosokawa F, Sakedai E 1997, *Inst. Phys. Conf. Ser.* **153**, 155
 Krivanek O, Kundmann MK and Kimoto K 1995, *J. Microsc.* **180**, 277